Science Press

ARTICLE

Stress Corrosion Cracking and Corrosion Fatigue Behavior of Micro-arc Oxidized Mg-3Al-1Zn Alloy

He Xiuli[1],   Yan Zhifeng[2],   Liang Hongyu[1],   Bai Rui[1],   She Yinzhu[1]

[1] Department of Mechanical Engineering, Taiyuan Institute of Technology, Taiyuan 030008, China; [2] Shanxi Key Laboratory of Advanced Magnesium-Based Materials, School of Materials Science and Engineering, Taiyuan University of Technology, Taiyuan 030024, China

Abstract: The stress corrosion cracking (SCC) and corrosion fatigue (CF) behaviors of micro-arc oxidized (MAO) Mg-3Al-1Zn alloy were investigated in air and 3.5 wt% Na_2SO_4 solution, and their relations were discussed. The corrosion properties of the MAO Mg-3Al-1Zn alloy were improved significantly. Compared with those of the Mg-3Al-1Zn substrate, the SCC and CF strengths of the MAO Mg-3Al-1Zn alloy were both reduced by only about 10 MPa slightly in air. In 3.5 wt% Na_2SO_4 solution, the CF properties were still degraded, but the SCC properties of the MAO specimens were enhanced apparently, from 58.24 MPa to 202.08 MPa. It indicated that the mechanical properties (SCC and CF) were not always linearly related with the corrosion resistance of the material. It was ductile fracture for the SCC specimens in air, and it was cleavage fracture in 3.5 wt% Na_2SO_4 solution. While they were cleavage fractures for CF specimens regardless of the environments. This was due to the effect of the corrosive environment and alternating cyclic loading, which accelerated the crack propagation process. It displayed that the surrounding environments and loading types could affect the fracture mechanism of the material.

Key words: Mg-3Al-1Zn alloy; micro-arc oxidation; stress corrosion cracking; corrosion fatigue; Na_2SO_4 solution

Magnesium alloys are anticipated in many areas such as electronic, structural, and automobile industries on account of their light weight, good formability and shock absorption ability[1,2]. However, the poor corrosion resistance of magnesium alloys limits the applications, especially for those serving under the joint action of stress loadings and corrosive environments. Stress corrosion cracking (SCC) and corrosion fatigue (CF) fractures are the two main failure forms of engineering structures, which restricts the wider use of magnesium alloys further. Therefore, to understand the relationship between corrosion and mechanical properties of magnesium alloys is crucial for the development of magnesium alloys.

In recent years, the corrosion, SCC and CF properties of magnesium alloys have been studied. Many factors affect the corrosion performance of magnesium alloys, such as types of environments[3,4], corrosion ways[5,6] (immersion and salt-spray etc.), compositions and microstructures[7-9].

Esmaily et al.[10] and Atrens et al.[11] reviewed the developments of corrosion properties of magnesium alloys. The vulnerability to corrosion is one of the inherent limitations for magnesium alloys.

Those factors affect the corrosion performance also have significant effect on the SCC performance of magnesium alloys commonly[12-15]. In addition, there are other factors affecting the SCC properties of magnesium alloys. Padekar et al.[16] studied the SCC properties of magnesium alloy under different stress loading state (plane strain and plane), the K_{ISCC} were different under the two different stress loading states. Uematsu et al.[17,18] considered the effect of potentials on the SCC properties of AZ31 magnesium alloy, and it is displayed that the SCC types occurred under different potential, which could be determined by K_{ISCC} factors. Rare earth elements also have an effect on the SCC properties of magnesium alloys, the K_{ISCC} was higher than that of magnesium alloys non-containing rare earth elements[19,20].

Harandi et al.[21] studied the effect of bovine serum albumin on the corrosion and SCC properties of AZ91D magnesium alloy. It reported that the bovine serum albumin helped to improve the corrosion resistance of the AZ91D magnesium alloy only in the first 48 h, and the SCC susceptibility was greater with the action of bovine serum albumin than that with none.

Similarly, those factors mentioned above also have important effect on the CF properties of magnesium alloys[22-26]. Besides, the effect of fatigue loading parameters (for instance, loading frequency *f* and stress ratio *r*) could not be ignored. He et al.[27-30] and Zeng et al.[31,32] investigated the effect of loading frequency on the CF behavior of magnesium alloys, and it is demonstrated that the fatigue limits of magnesium alloys at high frequency were higher than that obtained at low frequency. Klein et al.[33-36] investigated the CF behaviors of different creep-resistant magnesium alloys (DieMag422, AE42 and Mg-4Al-2Ba-2Ca). Results showed that the CF strength was lowered with the increasing corrosion impact, and the corrosion effect was closely related with the CF strength of magnesium alloys. Diab et al.[37] reported that the CF strength of AZ31B alloy was not improved with the Al coating, while the corrosion resistance of AZ31B alloy coated with Al was improved. Jafari et al.[38,39] studied the SCC and CF performances of magnesium alloys (AZ91D and MgZn1Ca0.3) in body fluid. It is illustrated that the SCC susceptibility of specimens after a calcium phosphate coating treatment could be weakened, but there was no obvious enhancement on the CF property. The SCC and CF properties of MgZn1Ca0.3 alloy were all deteriorated in body fluid.

Overall, the corrosion, SCC and CF performances of magnesium alloys are complex and interrelated, which need further research urgently for the security applications of magnesium alloys. To date, the micro-arc oxidation (MAO) method has been a commonly used method for the surface treatment of magnesium alloys[40-43]. This paper, on the basis of previous studies[27-30,44], is inspired and would systematically investigate the influences of the MAO coatings, surrounding environments and loading types on corrosion, SCC and CF performances of Mg-3Al-1Zn magnesium alloy, and explore their mutual relations.

1 Experiment

1.1 Materials and specimens

An extruded Mg-3Al-1Zn magnesium alloy (2.9 wt% Al, 0.9 wt% Zn, 0.3 wt% Mn, and Mg balance) was used in the experiment. The specimens (Φ12 mm×260 mm), with the gauge part size of Φ6 mm × 40 mm, were machined from the as-received round bar (Φ14 mm×260 mm). They were polished with 800#, 1000#, 1500# emery papers, cleaned with distilled water and wiped with acetone prior to the tests and MAO treatment. The corrosive environment was 3.5 wt% Na_2SO_4 solution for the corrosion, SCC and CF tests.

1.2 Coating preparation

The MAO coatings of Mg-3Al-1Zn magnesium alloy were prepared by the MAO160-II machine. The electrolyte consists of sodium silicate, potassium fluoride and potassium hydroxide, with the mass ratio of 2:1:1.25. The constant voltage and current density were 500 V and 0.3 A/cm^2, respectively. The oxidation time was 2 min. The Mg-3Al-1Zn magnesium alloy specimens after MAO treatment were called the MAO specimen in this paper.

1.3 Corrosion test

The corrosion resistance of the MAO specimens was tested by an electrochemical workstation (PGSTAT30). The saturated calomel electrode was used as the reference electrode, the platinum electrode was used as the counter electrode, and the specimen with the size of 10 mm × 10 mm was used as the working electrode. The scan range was from −2.0 V to 1.2 V. And the scan rate was 2 mV/s. The experimental results are compared with that of the Mg-3Al-1Zn substrate in the previous researches[44].

1.4 Slow tensile test

The SCC performance test of the MAO specimens was investigated on the slow tensile test machine (LETRY-WOML-10) with a corrosion tank (250 mL). According to ISO-7539-7-2005, the strain rate was adopted as 10^{-6} s^{-1}. During the test, the gauge part of the specimen was kept in corrosive environment in the corrosion tank. For comparison, the SCC test of the MAO specimens in air was also performed. The results are compared with those of the Mg-3Al-1Zn substrate in the air and 3.5 wt% Na_2SO_4 solution[44].

1.5 Corrosion fatigue test

The CF performance test of the MAO specimens was carried out by the high frequency tension-compression fatigue machine (PLG - 200D). During the whole fatigue test process, the gauge part of the specimen was kept in the corrosive environment in the corrosion tank, which was equipped on the fatigue machine. The fatigue test was performed by using a sinusoidal waveform at room temperature. The loading frequency and stress ratio were 99.0 Hz to 102 Hz and 0.1, respectively. Based on the relevant theories of fatigue life, the fatigue experiment would stop only when the specimen fractured or the number of cycles reached up to 1.0 × 10^7 cycle. Moreover, the maximum stress of the specimen sustained under the 1.0 × 10^7 cycle is called the fatigue limit. The results in the study were compared with those of the Mg-3Al-1Zn substrate in air and 3.5 wt% Na_2SO_4 solution[27, 28].

1.6 Other tests

The surface morphology and composition of the MAO coating were observed by scanning electron microscope (SEM VEGA3SBH), energy dispersive spectrometer (EDS,

OXFORD/ZNCA150) and X-ray diffraction (XRD, TD-3500). The fracture morphologies of the SCC and CF behaviors were observed by scanning electron microscope (SEM, VEGA3SBH).

2   Results

2.1   MAO coating observation

The surface morphology of the MAO coating is shown in Fig. 1a. It was flat and uniform. The composition of the MAO coating, marked by the rectangular area (Fig.1a), was analyzed by EDS as shown in Fig.1b. Na, Si, F and K elements were the main components of electrolyte, and it was the main source. C element was derived from the electro-conductive paste, which was formed during the preparation of the specimen. The main sources of O element were air and electrolyte. Mg, Al and Zn elements were from the substrate, which were the main components of Mg-3Al-1Zn alloy. To some extent, a significant reduction in the proportion of these three elements

indicated the formation of surface coatings.

The cross-sectional morphology of the MAO specimen was observed, as shown in Fig.2. It can be seen that the coating was smooth with uniform thickness, about 2.3 μm. A neat interface showed a good bonding between the coating and the Mg-3Al-1Zn substrate.

2.2   Corrosion characteristics

The potentiodynamic polarization curve of the MAO specimens in 3.5 wt% Na_2SO_4 solution is shown in Fig.3, and the polarization curve of the Mg-3Al-1Zn substrate in 3.5 wt% Na_2SO_4 solution was also included for comparison purpose[44] . The corresponding statistical data are listed in Table 1. According to the Tafel law, the corrosion potential of the MAO specimen was more than 100 mV higher than that of the Mg-3Al-1Zn substrate, and its corrosion current density was two orders of magnitude less than that of the Mg-3Al-1Zn substrate. It indicated that the corrosion resistance of the MAO specimen was significantly improved.

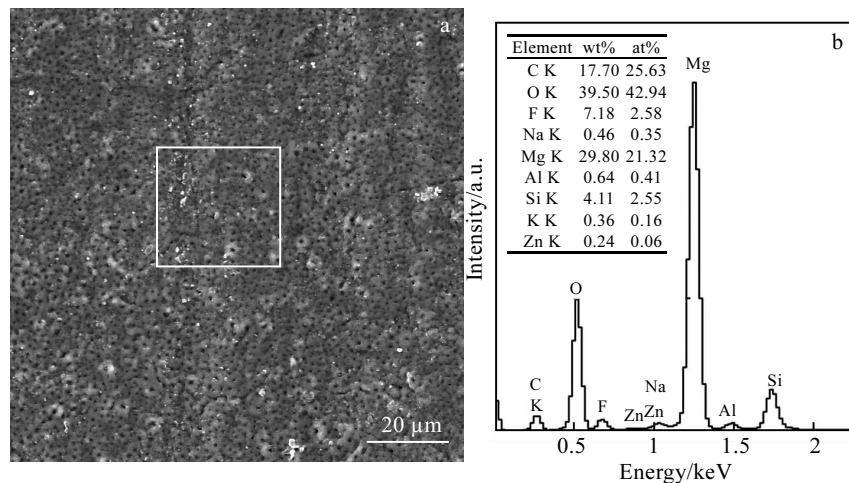| Element	wt%	at%
C K	17.70	25.63
O K	39.50	42.94
F K	7.18	2.58
Na K	0.46	0.35
Mg K	29.80	21.32
Al K	0.64	0.41
Si K	4.11	2.55
K K	0.36	0.16
Zn K	0.24	0.06

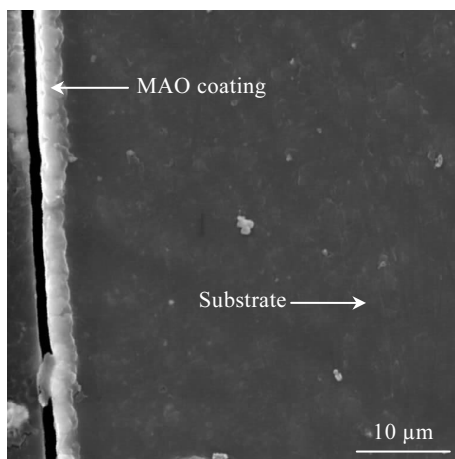Fig.1   Surface morphology (a) and EDS analysis results of the rectangular area (b) for the MAO coating

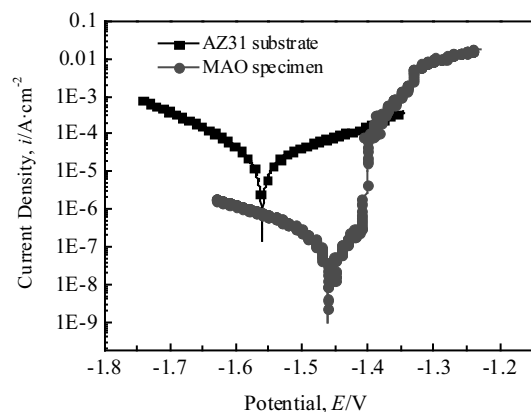Fig.2   Cross-sectional morphology of the MAO specimen

Fig.3   Potentiodynamic polarization curves of AZ31 alloy and MAO specimens in 3.5 wt% Na_2SO_4 solution

Table 1 Statistical data of the potentiodynamic polarization curve

Specimen	Potential, E_{corr} /V	Current density, i_{corr} /A·cm^{-2}
AZ31 substrate	−1.560	2.893×10^{-5}
MAO specimen	−1.457	3.348×10^{-7}

2.3 Stress-strain curves

The stress-strain curves of the MAO specimens in air and 3.5 wt% Na_2SO_4 solution after SCC tests were obtained and are shown in Fig.4. It can be seen from the figure that the Mg-3Al-1Zn alloy displayed the best SCC property in air, and the worst in 3.5 wt% Na_2SO_4 solution. After the coating treatment, the SCC performance of the MAO specimen was close to that of the Mg-3Al-1Zn alloy. The maximum tensile stress of the two was equivalent, the affordable strain was decreased due to the effect of the surface coating. However, in 3.5 wt% Na_2SO_4 solution, the SCC property of the MAO specimen was still much higher than that of the Mg-3Al-1Zn alloy because of the improved corrosion resistance.

2.4 *S-N* curves

The *S-N* curves of the MAO specimens in air and 3.5 wt% Na_2SO_4 solution after CF tests are shown in Fig.5, which displays the relation between the maximum applied stress σ_{max} and the number of cycles to failure *N* (fatigue life). It can be observed that the CF properties of the specimens before and after coating treatment were deteriorated apparently in 3.5 wt% Na_2SO_4 solution. In air, the CF property of Mg-3Al-1Zn alloy all decreased slightly after the MAO coating treatment.

2.5 Fracture surface observation

The fracture morphologies of the MAO specimens in air and 3.5 wt% Na_2SO_4 solution after SCC tests are shown in Fig.6. Fig.6a and 6b present the macroscopic integral fractures of the specimens and one amplified area of the crack initiations in air and 3.5 wt% Na_2SO_4 solution after SCC tests, respectively. It can be seen from the macroscopic

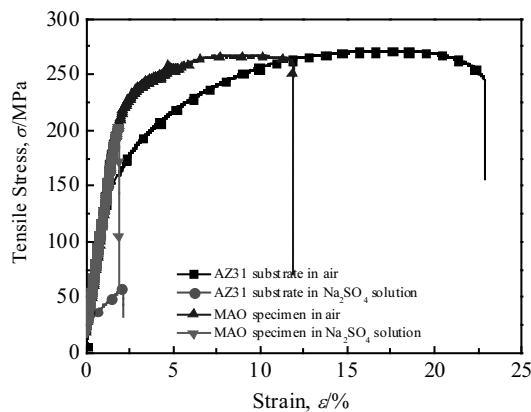Fig.4   Stress-strain curves of AZ31 alloy and MAO specimens in air and 3.5 wt% Na_2SO_4 solution after SCC tests

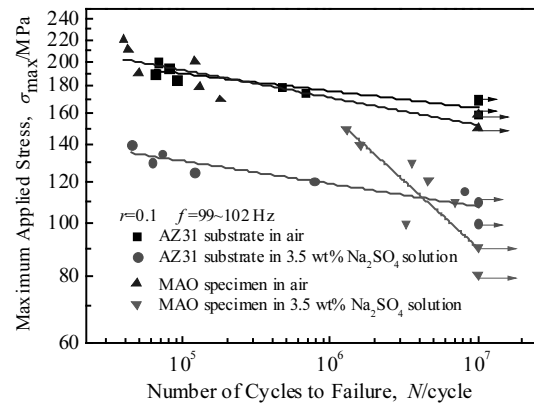Fig.5   *S-N* curves of AZ31 alloy and MAO specimens in air and 3.5 wt% Na_2SO_4 solution after CF tests

integral fractures (Fig.6a and 6b) that on the one hand, there were several crack initiations regardless of the environments as marked by ellipses in the figures. One of the crack initiations, area A and B, were magnified. It was observed that the cracks all initiated from the specimen surface, but the one in the air was relatively smooth, while that in the 3.5 wt% Na_2SO_4 solution was fuzzy and covered by some corrosion products. On the other hand, the two kinds of fractures were uneven, especially for that in air. To further observation, the rectangular areas of the fractures in air and 3.5 wt% Na_2SO_4 solution were magnified as shown in Figs.6c and 6d, respectively. There were many small dimples as marked by arrows (Fig.6c), which indicated a ductile fracture in air. While on the fractures in 3.5 wt% Na_2SO_4 solution in Fig.6d, some cleavage steps and secondary cracks as shown by arrows were observed, which are typical features of cleavage fracture. These were consistent with that of the Mg-3Al-1Zn substrate after SCC test[44], which demonstrated that the MAO coating had no influence on the mechanism of SCC fracture. By contrast, the crack propagation could be accelerated in corrosive environment, and the dimple had no enough time to be formed.

The fracture morphologies of the MAO specimens in air and 3.5 wt% Na_2SO_4 solution after CF tests are shown in Fig.7. Fig.7a and 7b present the macroscopic integral fractures of the specimens and the magnified crack initiations in air and 3.5 wt% Na_2SO_4 solution after CF tests, respectively. There were typical fatigue fractures, which included crack initiation, propagation and final fracture areas. And one crack initiation was observed, which was labelled by the ellipse mark. This was different from the SCC fractures (Fig.6a and 6b). The magnified crack initiations in air and 3.5 wt% Na_2SO_4 solution were similar, except that there were some corrosion products on the crack initiation surface in the latter. The rectangular areas (Fig.7a and 6b)
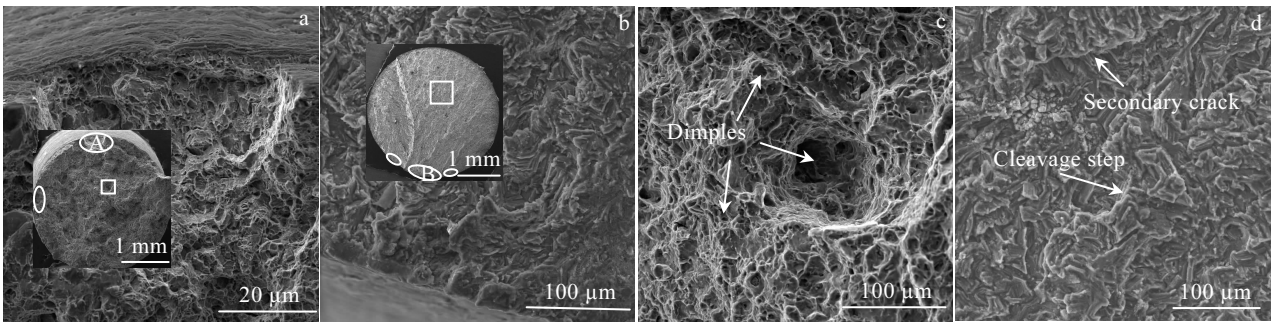
Fig.6   Fracture morphologies of the MAO specimens in air and 3.5 wt% Na_2SO_4 solution after SCC tests; macro and initiation zones in air (a) and 3.5 wt% Na_2SO_4 solution (b); crack propagation zones in air (c) and 3.5 wt% Na_2SO_4 solution (d)
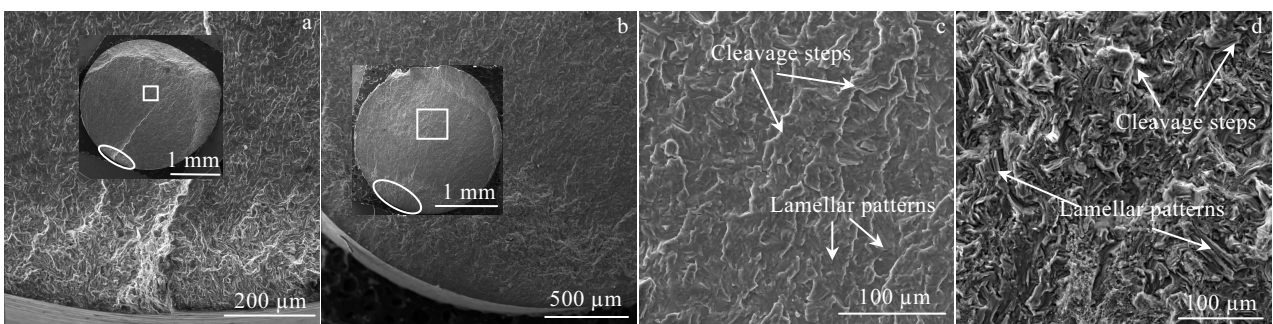

Fig.7   Fracture morphologies of the MAO specimens in air and 3.5 wt% Na_2SO_4 solution after CF tests; macro and initiation zones in air (a) and Na_2SO_4 solution (b); crack propagation zones in air (c) and 3.5 wt% Na_2SO_4 solution (d)

were magnified as shown in Figs.7c and 6d, respectively. There were some characteristics of cleavage fracture regardless of the environments, such as lamellar patterns and cleavage steps, as shown by arrows. The CF fractures of MAO specimens in air and 3.5 wt% Na_2SO_4 solution were all cleavage. These were consistent with that of the Mg-3Al-1Zn substrate[27,28], which indicated that the MAO coating and ambient environment had no effect on the mechanism of CF fracture. But it was different from the SCC fracture in air, which was ductile. It manifested that the mechanical fracture of materials was closely related to the state and type of the loading stress.

3   Discussion

3.1   Effect of corrosion on the SCC behavior of the MAO coated Mg-3Al-1Zn alloy

As stated previously, the corrosion resistance of the Mg-3Al-1Zn alloy after MAO coating treatment in 3.5 wt% Na_2SO_4 solution was enhanced significantly (Fig.3 and Table 1). The changes of the SCC properties of the MAO specimens were complicated as listed in Table 2.

In air, the maximum tensile stresses of the two kinds of specimens (the MAO specimen and the Mg-3Al-1Zn substrate) were close to each other, only decreased by about 10 MPa, but the maximum strain of the MAO specimen degraded about half compared with that of the Mg-3Al-1Zn substrate. This was due to the strengthening effect of the surface MAO coating. In 3.5 wt% Na_2SO_4 solution, the maximum strains of the two kinds of specimens showed little change, while the maximum tensile stress of the MAO specimen was improved apparently, about 2.5 times higher than that of the Mg-3Al-1Zn substrate. This was attributed to the evident improvement of corrosion resistance of the Mg-3Al-1Zn alloy after the MAO coating treatment. Overall, the SCC properties of the MAO specimens changed little in air, whereas it was improved significantly in 3.5 wt% Na_2SO_4 solution compared with that of the Mg-3Al-1Zn alloy. The effect of corrosion on the SCC behavior of the MAO coated Mg-3Al-1Zn alloy was related with the ambient environment. The positive effect of the good corrosion resistance on the SCC properties of the MAO specimens should be well played in 3.5 wt% Na_2SO_4 solution, not in air which is considered as the inert medium commonly.

According to the fracture morphologies (Fig.6), the fracture surface of the MAO specimens in air was rugged with lots of dimples, which showed the characteristics of the ductile fracture. While in 3.5 wt% Na_2SO_4 solution, it was relatively even. And there were secondary cracks and

Table 2 Data analysis of the SCC properties of the MAO specimens

Specimen	Environment	Maximum tensile stress, σ/MPa	Maximum strain, ε/%
AZ31 substrate	Air	276.23	22.73
	3.5 wt% Na_2SO_4 solution	58.24	2.11
MAO specimen	Air	266.74	11.87
	3.5 wt% Na_2SO_4 solution	202.08	1.89

cleavage steps on the fracture surface, which were the characteristics of cleavage fracture. On the one hand, compared with the fracture morphologies of the Mg-3Al-1Zn substrate, the fracture characteristics in air (ductile fracture) and 3.5 wt% Na_2SO_4 solution (cleavage fracture) were the same correspondingly[44]. It displayed that the good corrosion resistance of the MAO specimen could not change the SCC fracture mechanism of the Mg-3Al-1Zn alloy in the same environment. On the other hand, no matter coatings or not, it was cleavage fracture for the specimens in 3.5 wt% Na_2SO_4 solution, and ductile fracture in air after SCC tests. It was mainly because the corrosive environment not only accelerated the crack initiation, but also accelerated the crack propagation process, during which there was not enough time for the formation of dimples.

3.2 Effect of corrosion on the CF behavior of the MAO coated Mg-3Al-1Zn alloy

Based on the results after CF tests in section 2.4, the specific analysis results of the MAO specimens in air and 3.5 wt% Na_2SO_4 solution after CF tests are summarized in Table 3.

Compared with that of the Mg-3Al-1Zn substrate, the corrosion fatigue limit of the MAO specimens in air was slightly reduced by about 10 MPa, which could be ignored. It was in agreement with the changing trend of the SCC properties of the MAO specimens in air described above. However, in 3.5 wt% Na_2SO_4 solution, the corrosion fatigue limit of the MAO specimens was still decreased by about 17 MPa compared with that of the Mg-3Al-1Zn alloy. This was different from the results of the MAO specimens after SCC test mentioned above. It demonstrated that the improvement of the corrosion resistance could not enhance the CF properties, but improve the SCC properties of the MAO specimens in 3.5 wt% Na_2SO_4 solution. The effect of the corrosion on the different mechanical behaviors (SCC

Table 3 Data analysis of the CF properties of the MAO specimens

Specimen	Environment	CF limit, $\sigma_{0.1}$/MPa
AZ31 substrate	Air	163.89
	3.5 wt% Na_2SO_4 solution	107.51
MAO specimen	Air	152.55
	3.5 wt% Na_2SO_4 solution	90.24

and CF) of the MAO coated Mg-3Al-1Zn alloy was diverse.

As can be seen from the fracture morphologies (Fig.7), compared with those of the Mg-3Al-1Zn substrate[27, 28], the CF fracture characteristics of the Mg-3Al-1Zn alloy regardless of the MAO coating treatment, lamellar patterns and cleavage steps, were the same. There were three typical fatigue fracture zones including crack initiation, propagation and fracture zone. And there was only one crack initiation site for CF behavior of Mg-3Al-1Zn magnesium alloy. The corrosion and surface coatings could not affect the CF fracture mechanism. It was completely different from the SCC fracture morphologies.

3.3 Comparison between SCC and CF behavior of the MAO coated Mg-3Al-1Zn alloy

As aforementioned, compared with those of the Mg-3Al-1Zn substrate, the SCC and CF properties of the MAO specimens changed little in air. As can be analysed from the strength view (the maximum tensile stress and the corrosion fatigue limit), they both slightly decreased by about 10 MPa correspondingly. By contrast, the trend of the two was different in 3.5 wt% Na_2SO_4 solution. The SCC properties of the MAO specimens were much higher than those of the Mg-3Al-1Zn substrate in 3.5 wt% Na_2SO_4 solution, and the maximum tensile stress increased from 58.24 MPa to 202.08 MPa. While the CF properties of the MAO specimens were not enhanced compared with those of the Mg-3Al-1Zn substrate in 3.5 wt% Na_2SO_4 solution, and the corrosion fatigue limit was reduced by 17.27 MPa. The change trend of the SCC properties of the MAO coated specimens was consistent with that of the corrosion property of the Mg-3Al-1Zn alloy after MAO coating treatment, whereas it was adverse between the CF and corrosion properties. It was accordant with the trend referred in Ref. [37-39], but not in good agreement with that described in Ref. [21, 27-30]. It demonstrated that the effect of the corrosion on the mechanical properties of materials was related with many factors, such as the types of surface coatings and the state of the loading stress.

In the study, the state of the loading stress under SCC and CF test was different. During the SCC experiment, the specimens undertook a unidirectional tensile stress, and the strain rate was adopted as only 10^{-6} s^{-1}. It was so slow that the defects, formed by the corrosion reactions, could be covered by the corrosion products quickly, thus protecting

the substrate well. Then the SCC properties of the Mg-3Al-1Zn alloy after MAO coating treatment were improved apparently.

While for the CF process, the loading frequency and stress ratio were 99.0 Hz to 102 Hz and 0.1, respectively, which demonstrated that the specimens undertook a tension-tension alternating cyclic loading. It made the corrosion product layers, formed on the specimen surface in corrosive environment, fall off easily during the fatigue test, which helped protecting the substrate from the ambient corrosive environment. Then, the defects covered by the corrosion products were exposed effortlessly. The stress concentration was easily generated under the action of alternating loading, and these defects became the initiation source of corrosion fatigue crack. Thus, the CF properties of the MAO coated Mg-3Al-1Zn alloy were degraded, though there was a good corrosion resistance of Mg-3Al-1Zn alloy after MAO coating treatment.

4　Conclusions

1) The corrosion properties of the Mg-3Al-1Zn alloy after MAO coating treatment were improved significantly. Compared with those of the Mg-3Al-1Zn substrate, the SCC and CF strengths of the MAO coated Mg-3Al-1Zn alloy were both reduced by about 10 MPa slightly. By contrast, in 3.5 wt% Na_2SO_4 solution, the SCC properties of the MAO coated Mg-3Al-1Zn alloy were enhanced, but the CF properties were still degraded. The mechanical properties (SCC and CF) and the corrosion resistance were not linearly related.

2) There were several crack initiation sites for the SCC behavior, but only one for the CF behavior. It was ductile fracture for the SCC specimens in air, but cleavage fracture for the SCC specimens in 3.5 wt% Na_2SO_4 solution and CF specimens in the two environments. The corrosive environment and alternating cyclic loading accelerated the crack propagation process, during which there was no enough time for the formation of the dimples. It displayed that the surrounding environments and loading types could affect the fracture mechanism of the material.

References

1　Abbott T B. *Corrosion Protection of Magnesium and Magnesium Alloys*[J], 2015, 71(2): 120

2　You S H, Huang Y D, Ulrich K K *et al. Journal of Magnesium and Alloys*[J], 2017, 5(3): 239

3　Han L Y, Li X, Bai J *et al. Materials Chemistry and Physics*[J], 2018, 217: 300

4　Qu Q, Ma J, Wang L *et al. Corrosion Science*[J], 2011, 53(4): 1186

5　Martin H J, Horstemeyer M F, Wang, P T. *Corrosion Science*[J], 2010, 52(11): 3624

6　Shi Z, Cao F, Song G L *et al. Corrosion Science*[J], 2013, 76: 98

7　Hu Z, Liu R L, Kairy S K *et al. Corrosion Science*[J], 2019, 149: 144

8　Esmaily M, Blücher D B, Svensson J E *et al. Scripta Materialia*[J], 2016, 115: 91

9　Liao J S, Hotta M. *Corrosion Science*[J], 2015, 100: 353

10　Esmaily M, Svensson J E, Fajardo S *et al. Progress in Materials Science*[J], 2017, 89: 92

11　Atrens A, Song G L, Liu M *et al. Advanced Engineering Materials*[J], 2015, 17(4): 400

12　Zhou L F, Liu Z Y, Wu W *et al. International Journal of Hydrogen Energy*[J], 2017, 42(41): 26 162

13　Cao F Y, Shi Z M, Song G L *et al. Corrosion Science*[J], 2015, 98: 6

14　Cao F Y, Shi Z M, Song G L *et al. Corrosion Science*[J], 2015, 96: 121

15　Choudhary L, Singh Raman R K, Hofstetter J *et al. Materials Science and Engineering: C*[J], 2014, 42: 629

16　Padekar B S, Raja V S, Singh Raman R K. *Engineering Fracture Mechanics*[J], 2013, 102: 180

17　Uematsu Y, Kakiuchi T, Nakajima M. *Materials Science and Engineering A*[J], 2012, 531: 171

18　Uematsu Y, Kakiuchi T, Nakajima M. *Procedia Engineering*[J], 2011, 10: 578

19　Wang S D, Xu D K, Han E H *et al. Journal of Magnesium and Alloys*[J], 2014, 2(4): 335

20　Padekar B S, Raja V S, Singh Raman R K *et al. Materials Science and Engineering A*[J], 2013, 583: 169

21　Harandi S E, Banerjee P C, Easton C D *et al. Materials Science and Engineering C*[J], 2017, 80: 335

22　Khan S A, Bhuiyan M S, Miyashita Y *et al. Materials Science and Engineering A*[J], 2011, 528(4-5): 1961

23　Chamos A N, Pantelakis S G, Spiliadis V. *Materials & Design*[J], 2010, 31(9): 4130

24　Zeng R C, Han E H, Ke W *et al. International Journal of Fatigue*[J], 2010, 32(2): 411

25　Bhuiyana M S, Mutoh Y, Murai T. *Engineering Fracture Mechanics*[J], 2010, 77(10): 1567

26　Ishihara S, Nan Z Y, Naamito T *et al. Key Engineering Materials*[J], 2010, 452-453: 321

27　He X L, Wei Y H, Hou L F *et al. Proceedings of the Institution of Mechanical Engineers, Part C: Journal of Mechanical Engineering Science*[J], 2014, 228: 1645

28　He X L, Wei Y H, Hou L F *et al. Theoretical and Applied Fracture Mechanics*[J], 2014, 70: 39

29　He X L, Wei Y H, Hou L F *et al. Transactions of Nonferrous Metals Society of China*[J], 2014, 24(11): 3429

30　He X L, Wei Y H, Hou L F *et al. Rare Metals*[J], 2014, 33(3): 276

31　Zeng R C, Ke W, Han E H. *International Journal of Fatigue*[J], 2009, 31(3): 463

32　Wang B J, Xu D K, Wang S D *et al. International Journal of*

Fatigue[J], 2019, 120: 46

33 Klein M, Frieling G, Walther F. *Engineering Fracture Mechanics*[J], 2017, 185: 33

34 Klein M, Walther F. *Procedia Engineering*[J], 2016, 160: 158

35 Wittke P, Klein M, Dieringa H *et al. International Journal of Fatigue*[J], 2016, 83: 59

36 Wittke P, Klein M, Walther F. *Procedia Engineering*[J], 2014, 74: 78

37 Diab M, Pang X, Jahed H. *Surface and Coatings Technology*[J], 2017, 309: 423

38 Jafari S, Singh Raman R K. *Materials Science and Engineering C*[J], 2017, 78: 278

39 Jafari S, Singh Raman R K, Davies C H J *et al. Journal of the*

Mechanical Behavior of Biomedical Materials[J], 2017, 65: 634

40 Seyfoori A, Mirdamadi S, Mehrjoo M *et al. Progress in Natural Science: Materials International*[J], 2013, 23(4): 425

41 Seyfoori A, Mirdamadi S, Khavandi A *et al. Applied Surface Science*[J], 2012, 261: 92

42 Yang W, Xu D P, Wang J L *et al. Corrosion Science*[J], 2018, 136: 174

43 Yang W, Xu D P, Yao X F *et al. Journal of Alloys and Compounds*[J], 2018, 745: 609

44 He X L, Yan Z F, Liang H Y *et al. Journal of Materials Engineering and Performance*[J], 2017, 26: 2226

微弧氧化 Mg-3Al-1Zn 镁合金应力腐蚀和腐蚀疲劳行为研究

贺秀丽 [1]，闫志峰 [2]，梁红玉 [1]，白 瑞 [1]，佘银柱 [1]

(1. 太原工业学院 机械工程系，山西 太原 030008)

(2. 太原理工大学 材料科学与工程学院 山西省先进镁基材料重点实验室，山西 太原 030024)

摘　要：主要对微弧氧化 Mg-3Al-1Zn 镁合金在空气和 3.5%硫酸钠溶液 2 种环境下的应力腐蚀和腐蚀疲劳行为进行研究，并讨论其相互关系。微弧氧化处理后，Mg-3Al-1Zn 镁合金的耐蚀性能得到明显改善。与 Mg-3Al-1Zn 镁合金基体相比，在空气中，微弧氧化后合金的应力腐蚀和腐蚀疲劳强度均下降了大约 10 MPa。在 3.5% 硫酸钠溶液环境中，微弧氧化后合金的腐蚀疲劳性能仍然是恶化的，但是应力腐蚀强度却得到了显著改善，从 58.24 MPa 提高至 202.08 MPa。这表明材料的力学性能（应力腐蚀和腐蚀疲劳）并不是与其腐蚀性能完全保持线性关系的。微弧氧化处理后镁合金在空气中的应力腐蚀断口为韧性断裂，在硫酸钠溶液环境中为解理断裂。而其腐蚀疲劳断口不论是在空气中还是在腐蚀环境中均为解理断裂。这主要是由于腐蚀环境和变换循环载荷的影响，两者共同作用将会加速裂纹扩展。这表明，周围环境和加载类型对材料断裂机理有重要影响。

关键词：Mg-3Al-1Zn镁合金；微弧氧化；应力腐蚀；腐蚀疲劳；Na_2SO_4溶液

作者简介：贺秀丽，女，1985 年生，博士，副教授，太原工业学院机械工程系，山西 太原 030008，电话：0351-3566033，E-mail: good.168@126.com